THE F2 WIND TUNNEL OF THE FAUGA-MAUZAC TEST CENTER

ICAS-86-1.7.4

J.M Christophe
Deputy Director large testing facilities department

Office National d'Etudes et de Recherches Aérospatiales
BP.72 , 92322 Châtillon Cedex , France

Abstract

The new subsonic wind tunnel F2 devoted to research programs was operated at the first on july 1983. It is concerned with the detailed survey of aerodynamic flows using the most modern technics.

Due to the continuous increase in the calculation power of the computers and to the improvements of numerical calculations in theoretical aerodynamics it is possible to study more and more sophisticated 2D and 3D flows.

However, mathematic models and results must be validated by tunnel tests using as well more and more sophisticated test technics in order to get detailed analysis of the flows.

So, the calculation-experiment interaction becomes a fruitful mean to help for the best airplane design and also for fundamental phenomena understanding.

This wind tunnel, which the test section is 1.4 m x 1.8 m and the length 5 m, and which can be run at a speed up to 100 m/s has been described in previous papers. Thus the only main characteristics are reminded in the present paper.

A first part describes the laser velocimeter system which is a basic equipment designed in close connection with the test section of the tunnel.This device can explorate a volume of 1.4 x 1.8 x 4.25 m^3 with displacements of $\pm$ 0.25 m axial ; $\pm$ 0.3 m lateral ; $\pm$ 0.5 m vertical.

A second part gives the main results of the aerodynamic calibration.

At least, in the third part, some examples of results obtained are presented.

I.Introduction

During the last decades the progress of computer was exponential, from an effective computing speed of 10^{-2} megaflops in 1955 to 10 in 1975 (and an expected value to about 10^4 megaflops in the late 1990 s). In the same period the increase of memory was from 10^4 words in 1955 to 10^6 in 1975 (reaching an expected value about 500.10^6 words in the late 1990s) (5 pages 7, 58, 59, 70 and 73).

This enormous development and the large development in the field of numerical mathematics gave a large impetus to computational fluid dynamics. Thus the largely increased capability of computational fluid dynamics becomes integrated in aerodynamic research, interpretation and analysis of wind tunnel data, design and development of aircraft.

This evolution challenges the respective uses of wind tunnel and computational fluid dynamics (1 to 8) .But contrary to some predictions the rapid progress in computer technology and computational fluid dynamics experienced in the last few years, is acting as a stimulant to the wind tunnel (8). An optimal result can only be obtained by a well- balanced use of computation and experiment. Ultimate goal is not to replace the wind tunnel by a computer, but to use both disciplines in a complementary sense, in order to take advantage of the merits of both (4). This synergistic approach appears very clearly concerning the requirements for code verification(9)

The figure 1 shows a general view of the main stages of approximation to three dimensional numerical aerodynamic simulations in computational fluid dynamics each representing the employment of a successively refined approximation of the full Navier-Stokes equations that govern fluid motion (5,6).

STAGE		APPROXIMATION	COMPUTER CLASS FOR PRACTICAL 3D ENGINEERING COMPUTATIONS
I PAST	INVISCID LINEARIZED (1960's)	VISCOUS AND NONLINEAR INVISCID TERMS NEGLECTED	IBM 360 CDC 6600
II PRESENT	INVISCID NONLINEAR (1977)	VISCOUS TERMS NEGLECTED	CDC 7600 STAR CRAY ILLIAC IV
III NEXT STEP	REYNOLDS TIME AVERAGED NAVIER STOKES (EARLY 1980's)	NO TERMS NEGLECTED TURBULENT MOMENTUM AND HEAT TRANSPORT TERMS MODELED	AT LEAST 40 TIMES CURRENT SUPERCOMPUTERS
IV FAR FUTURE	FULL TIME DEPENDENT NAVIER STOKES (CIRCA 1990)	SUB GRID SCALE TURBULENCE MODELED	AT LEAST 100 TIMES REQUIREMENT FOR STAGE III

Figure 1. Stages of approximation to three-dimensional numerical aerodynamic simulations.

Uncertainties arising from transition and turbulence modeling form the primary limitations of the stage of computation III, notable progress should be made in the coming 10 to 15 years but it is not anticipated that the problem of turbulence modeling will then be fully solved (5)

On the other hand confidence in the computed results for complex separated flows, such as those about fighter aircraft operating at large angles of attack, does not now exist.

The need for establishing confidence in the use of computational fluid dynamics for predicting complex flows requires experimental effort. The document (9) considers two main requirements. The first of these requirements involves experiments to establish phenomenological input for situation in which understanding of the flow physics is limited. The second requirement involves experiments that establish the confidence limits on computational fluid dynamics predictions of complex flows over parametric variations.

The figure 2, given in(9), is a framework for discussing experimental requirements and shows three stages : "building block" experiments considering phenomenological studies, "benchmark" parametric testing over the full range of flight Mach numbers and Reynolds numbers, "design experiments" requiring the use of the larger national facilities.

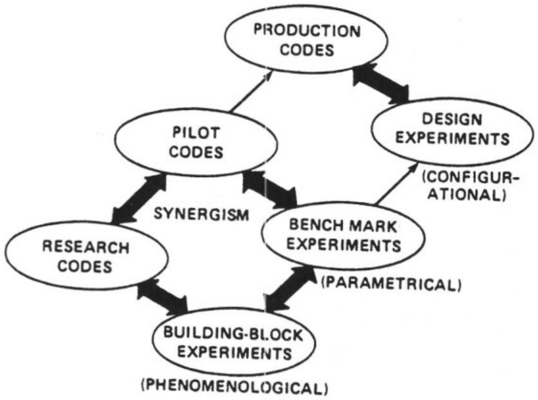

Figure 2. The role of experiment in the development of CFD.

The wind tunnel F2, devoted to research programs, may be classified in the stage "building block" experiments at incompressible flow conditions.

II. F2 Subsonic Research Wind Tunnel

The research wind tunnel F2 (10, 11, 12) was built, at the Fauga-Mauzac Center, near the large pressurized subsonic wind tunnel F1 (test section 3.5 m x 4.5 m ; stagnation pressure up to 4 bar) devoted to industrial tests with a portion of research tests.

The figure 3 gives an aerial view of F1 and F2 and the general layout of F2 is given by the figure 4.

This continuous wind tunnel is driven by a fan with constant blade angle and a variable speed motor with a power up to 700 kW.

The air speed is variable from 0 to 100 m/s.

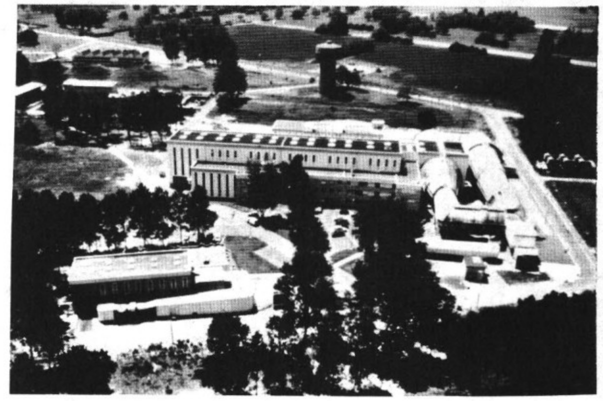

Figure 3. Aerial view F1 on the right, F2 on the left.

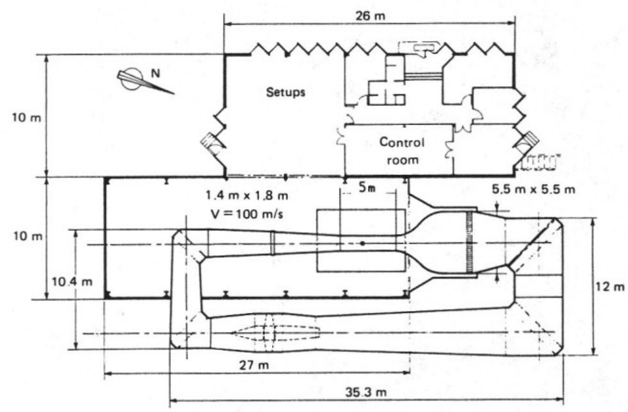

Figure 4. Aerodynamic circuit and technical support rooms.

The stagnation pressure is atmospheric pressure.

The test section is rectangular : height 1.80 m, width 1.40 m length 5 m.

The contraction ratio is 12.

The stilling chamber is equipped, following the wind, with a net in the rapid expansion, an honeycomb and three nets.

The water cooler is placed between the corner 3 and the corner 4.

The cooler section, the fan section, the corner vanes, and the central section including : contraction, test section and the beginning of the first diffusor are built in steel. The rest of the tunnel is in concrete.

The wind tunnel is intended for use in the basic experimental subsonic research of the ONERA Aerodynamics Department and of the CERT AerothermodynamicsDepartment. So the test section area was designed to provide the experimenters with the best possible working conditions and to reach a large versatility for setting the models and for instrumentation intrusive and non intrusive. The lateral walls of the test sections are easy to disassemble, they are opaque or transparent as needed (figure 5).

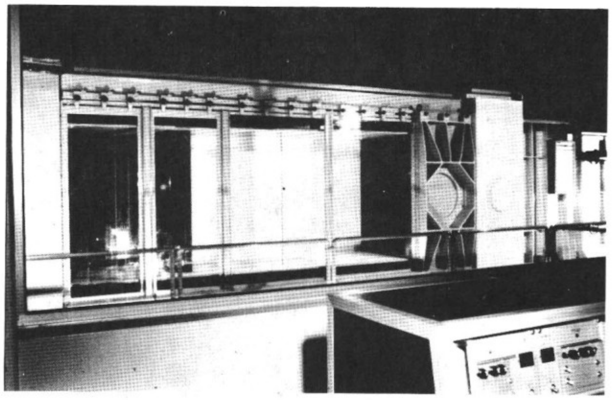

Figure 5. Test section seen from the wind tunnel operation room.

The test section is surrounded by a large movable rigid gantry able to support various optical systems to aim at any point of the flow through the glass panels of the test section (figure 6 and figure7).

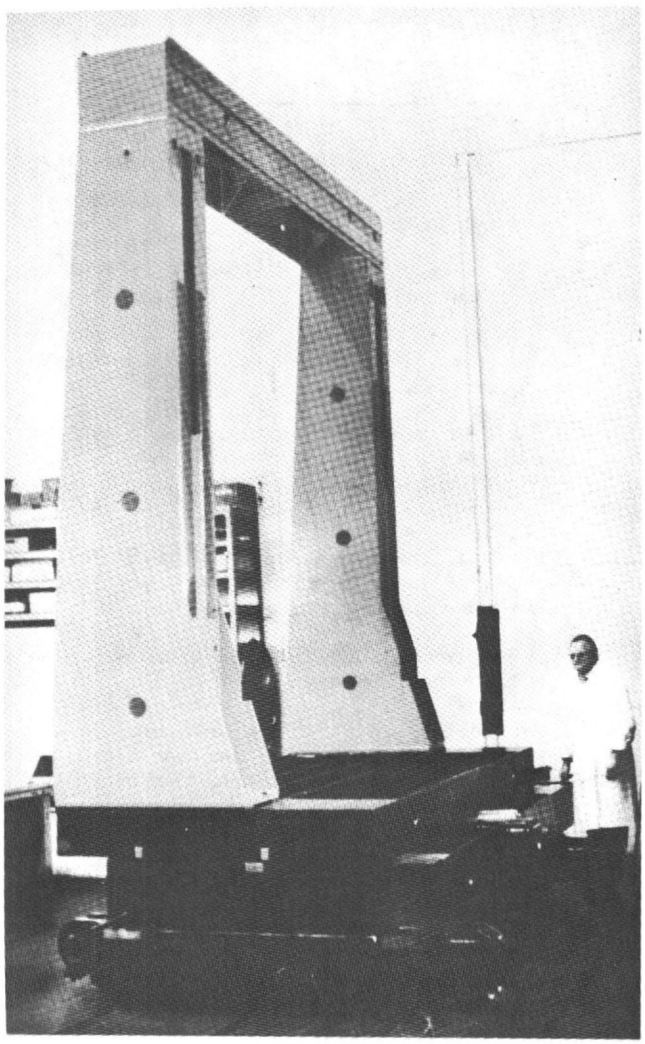

Figure 7. Photography of the gantry (velocimeter support) in the workshop during acceptance tests.

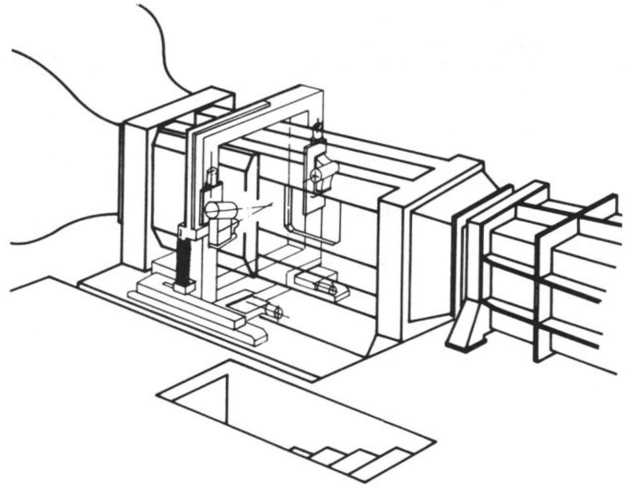

Figure 6. Test section and mobile velocimeter support.

At this time the gantry supports optics for laser tomography and 2 D laser velocimetry.

III. The Optical Flow Analysis Systems

The instrumentation support is equipped with a coarse displacement drive X_G, with a 3.75 m course of travel (X is the horizontal axial centerline of the wind tunnel in the direction of the average wind with the section empty, Y is the horizontal axis perpendicular to X and Z is the vertical axis). A "fine" mechanism of translation along Y extending over 600 mm is mounted above X_G as shown in figure 8 along with a "fine" X movement extending over 500 mm. A rugged structure in the form of an upside-down U rests on this fine X drive. Two slides are mounted on the legs of the U to guide the motion 1 m in the Z direction.

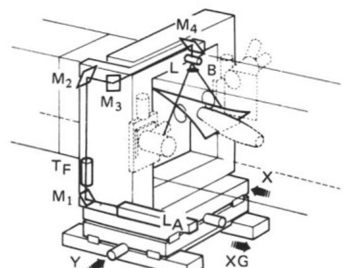

8a

Tomography

M_1 ...M_4 : Dielectric mirrors
T_F : Focusing telescope
B : Cylindrical lens
L : Lens

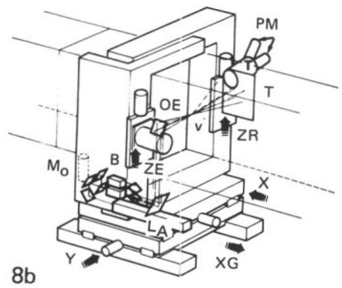

8b

Courses of travel
X : ± 0.250 m
Y : ± 0.300 m
ZE, ZR : ± 0.500 m
XG : 3.750 m

Two-dimensional velocimetry
V : Probe volume
T : Receiver telescope
PM : Photomultiplier
OE : Emission optics
B : Beam splitter
Mo : Retractable mirror
LA : 9 W Argon laser.

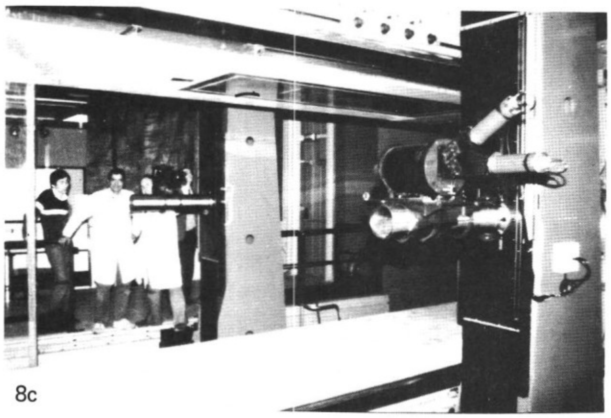

8c

Figure 8. Laser velocimetry and tomography device (8a tomography - 8b velocimetry - 8c photography, in the foreground the receiver telescope).

Two types of optical instruments have been installed : a 2-D laser velocimeter, planned for 3-D extension in the near future, and a laser sheet visualization device. A single argon laser, emitting 9 W all lines, is used for both optical techniques. To use the laser velocimeter function, a retractable mirror M_0 can be inserted in the light path as shown in figure 8b. When M_0 is switched off the laser beam follows the path shown in figure 8a up to mirror M_2 overhead the wind tunnel, and is then sent to the cylindrical lens that spreads it out into a vertical plane, which can be rotated about a vertical axis. T_0 is an "afocal" telescope which, by a slight adjustment of the distance between its two lenses, compensates for the divergence of the laser beam at the level of the cylindrical lens. This light sheet can thus be moved 4.25 m along the X axis and 0.6 m along the Y axis.

The optical diagram of the 2-D velocimeter is given figure 9. Its essential characteristic is that it has two independent (green and

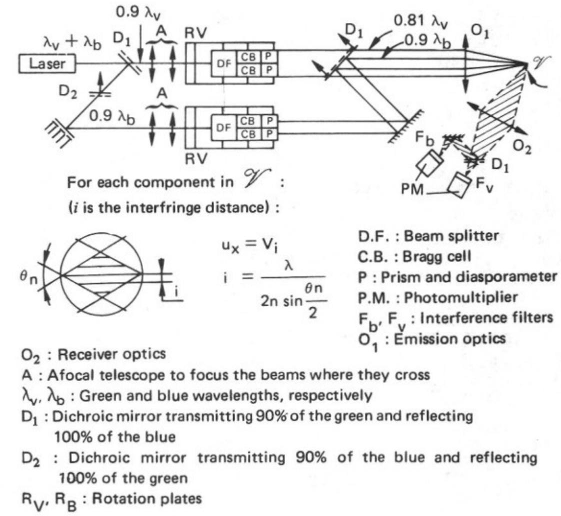

Figure 9. Optical diagram.

blue) beam splitter channels, in preparation for a possible extension to space-time correlation techniques. Acoustooptical modulators are placed in each channel to make the fringe pattern move at preset frequencies from 2.5 MHz to 15 MHz (for analyzing very turbulent flows).

The beam splitter and laser assembly can be moved in the X and Y directions. The four green-blue beams are then directed up to the emission optics, which can only be moved in the Z direction (Figure 8b). The instrumentation mechanical support sets the optical probe volume with an accuracy of the order of 0.1 mm.

The receiver is a Cassegrain telescope with a 200 mm primary mirror and aperture varying from F/5 to F/8. This telescope can be set up in the backscattering mode (on the same slide as the transmitter optics) or in the forward scattering mode on the Z slide on the opposite side of the test section. The latter configuration produces the best signal/noise ratio, but cannot always be used in the presence of a model (figure 8c).

The two photomultiplier output signals are processed by classical counting techniques with a simultaneity criterion. The instantaneous frequency pairs from the counters defining the instantaneous local velocity vector are sent to the computer for all of the usual statistical processing giving the mean components of the velocity ($\bar{u}$, $\bar{v}$) and the various turbulence parameters ($\bar{u'^2}$, $\bar{v'^2}$, $\bar{u'.v'}$).

Thus the computer handles the whole experiment automatically :

- acquisition of initial conditions (pressure and temperature),
- acquisition and processing of the velocimeter data,
- displacement of the probe volume according to a preprogrammed mapping.

Currently, the flow is seeded by smokes of filtered incense injected downstream of the test section. These aerosols continue through the entire circuit, homogeneously seeding the flow and providing an acquisition rate of several kilohertz in forward scattering mode, with a particle size distribution of 0.5 to 0.8 μm.

This optical system was designed by the ONERA Physics Department which has acquired a large expertise of the laser velocimetry in wind tunnel (13 to 17) in close connection with the ONERA Aerodynamics Department.

At this time the improvement from 2D to 3D is in process of completion thanks to a study made together by Physics Department and Large Testing Facilities Department.

IV. Flow Calibration

A preliminary aerodynamic test phase gave the essential characteristics of the flow in the test section and in many sections of the circuit. It showed that the expected performance was achieved.

Tests to characterize the test section flow, more finely, have been pursued.

The homogeneity of the flow velocity V in various transversal plane of the section was explored successively with laser velocimetry, pressure probe and hot-wire. The pressure probe and the hot-wire were supported by a three degrees of freedom device (X horizontal axial centerline, Y and Z) fastened to the test section inside.

The figure 10, obtained by pressure probe gives the comparison of the local values V, in a vertical plane located 1 meter behind the beginning of the test section, and the reference value Vomeasured by a fix pressure probe located 0.786 m behind the beginning of the test section and 0.3 m under the upper wall ; in this case Z = 0.902 m and Y = 0.798 m and Vo = 100 m/s. This figure shows a very good homogeneity in the plane.

The laser accuracy was estimated to a relative error $\Delta V/V <$ 1,5% and an absolute error on the angle between speed and an horizontal line 0.5 degree. These measurements show the same homogeneity that the pressure measurements and the measured angles were always smaller than the estimated error. The hot wire measurements, although disturbed by small mechanical vibrations of the supporting device, shows the same uniformity of the flow. Dynamics measurements of pressure fluctuations $\bar{p}'^2$ and speed fluctuation $\bar{u}'^2$ were made by a microphone and a hot wire in the test section.

A quarter inch Bruel and Kjaer microphone equipped with a cone (16 k Hz pass band) was placed 3.6 m from the test section inlet on the horizontal axial centerline. The values of $\sqrt{\bar{p}'^2}$ were obtained without filtering (figure 11).

An horizontal 5 μ m hot wire was placed 0.8m from the test section inlet and 0.2 m from the upper wall. The values of $\sqrt{\bar{u}'^2}$ were determined in the 0 to 1 000 Hz frequency band (figure 12).

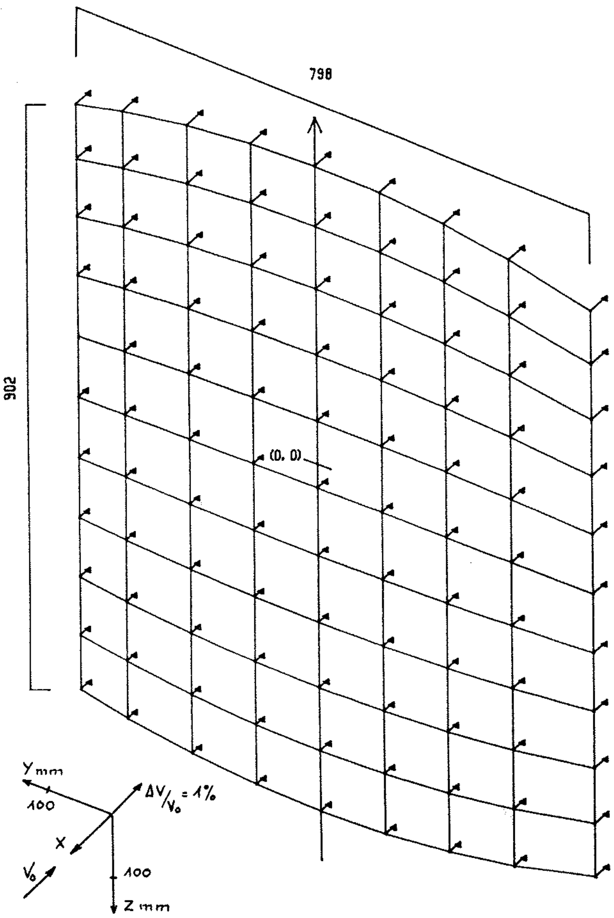

Figure 10. Transversal survey in the test section.

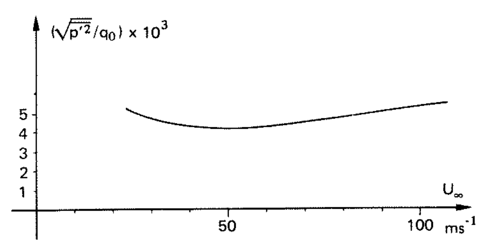

Figure 11. Fluctuation of the static pressure.

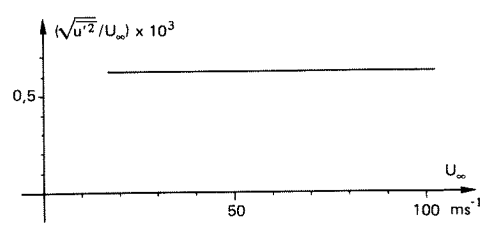

Figure 12. Axial turbulence.

V. Some Samples Of Results

We will give now some typical results among different tests. For all tests the very good symmetry of the flow obtained confirms the quality of the flow in the wind tunnel.

V.1. 2D Cylinder

An horizontal cylinder is placed between the two vertical walls of the wind tunnel for a 2D test. This test was simultaneously a sort of "bench mark" for the wind tunnel, using pressure measurement, friction tranducer, wake study with laser and with hot wire, and a research test. The cylinder is equipped with a friction transducer and three pressure holes. The rotation around the axis of the cylinder gives the evolutions of the measurements with the angular position. One hole is at the intersection between a generating line and the vertical plane in the middle of the test section, the two other holes are on the opposite generating line at the same distance of the vertical plane, one on the right the other on the left. So the experimenter can see if the flow is really 2D. The figure 13 shows the pressure evolution expressed in the form V/Vo, for V_o = 40 m/s and 80 m/s the ordinates of the three curves are shifted to avoid a mixing of the dots.

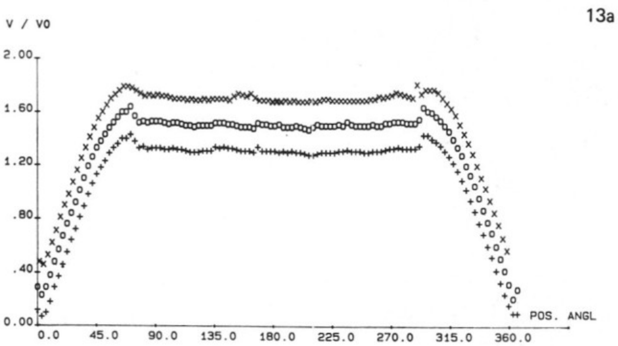

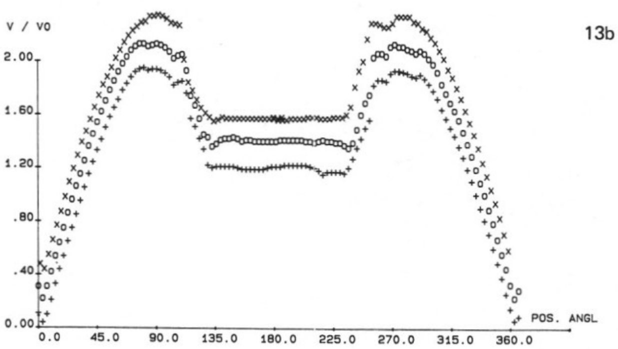

Figure 13. Pressure distribution on the cylinder (13a 40m/s, 13b 80m/s, +, 0 are on a generating line, X is on the opposite generating line, origin ordinate shift 0.20).

The figure 14 gives the shear stress measured by a friction transducer and computed with the experimental evolution of pressure for a laminar boundary layer.

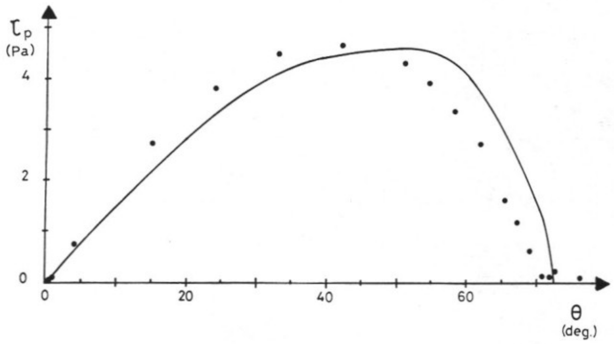

Figure 14. Shear stress (30 m/s, • experimental, —— computational).

V.2. Elliptical Body Tests For The Understanding Of 3D Separation

The Aerodynamics department performed, since 1983, series of tests on elliptical bodies for a fundamental research on tridimensionnal separation. The aim of those tests is to define and to validate theoretical models.

An axisymmetrical body (total lenght 1.83 m) with an elliptical nose (half axis 0.8 m and 0.2 m) followed by a cylinder (diameter 0.4 m) was tested in F_2, in 1985, from 0 to 90 m/s, up to pitch angle 40 degrees (figure 15). The body is equipped with 278 pressure holes.

The tests without yaw showed an excellent symmetry of the pressures between the right and the left sides, up to 40 degrees.

Between 10 and 20 degrees symmetrical vortices appear The Cp curves at 0 and 10° are exactly the same for V_o = 30 m/s, 60 m/s and 90 m/s. From 20° to 40° the Cp curves vary with the speed (Reynolds number effect).

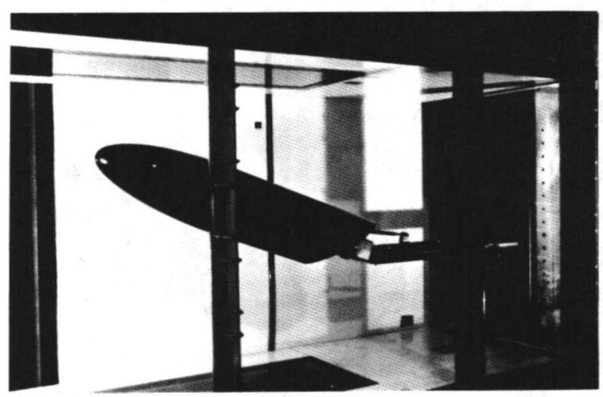

Figure 15. Elliptical body in the test section.

The figure 16 shows the Cp distribution at 40°, 90 m/s (the reference lenght L = 1.60 m). The flow on the skin of the body, visualized by an oil coating, shows the separation and attachment lines, which appears clearly on the figure 17. This shows three photographies :
a front view following F" (fig 18), a vertical view along F, a detail of the rear part of the body along F'. The test conditions are 40° and 90 m/s.

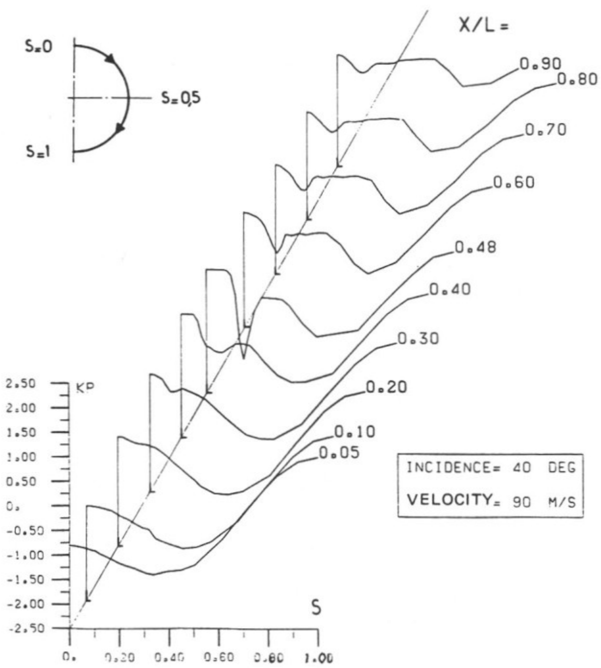

Figure 16. Distribution of the pressure coefficient (V_o = 90m/s, pitch angle 40°).

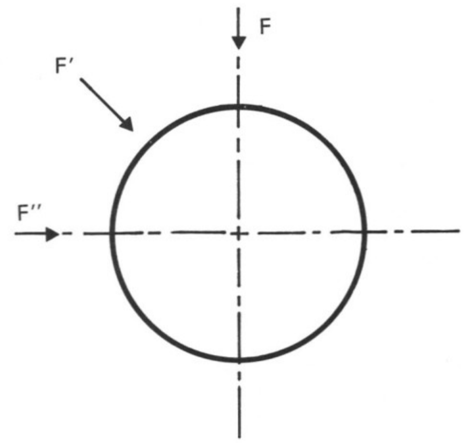

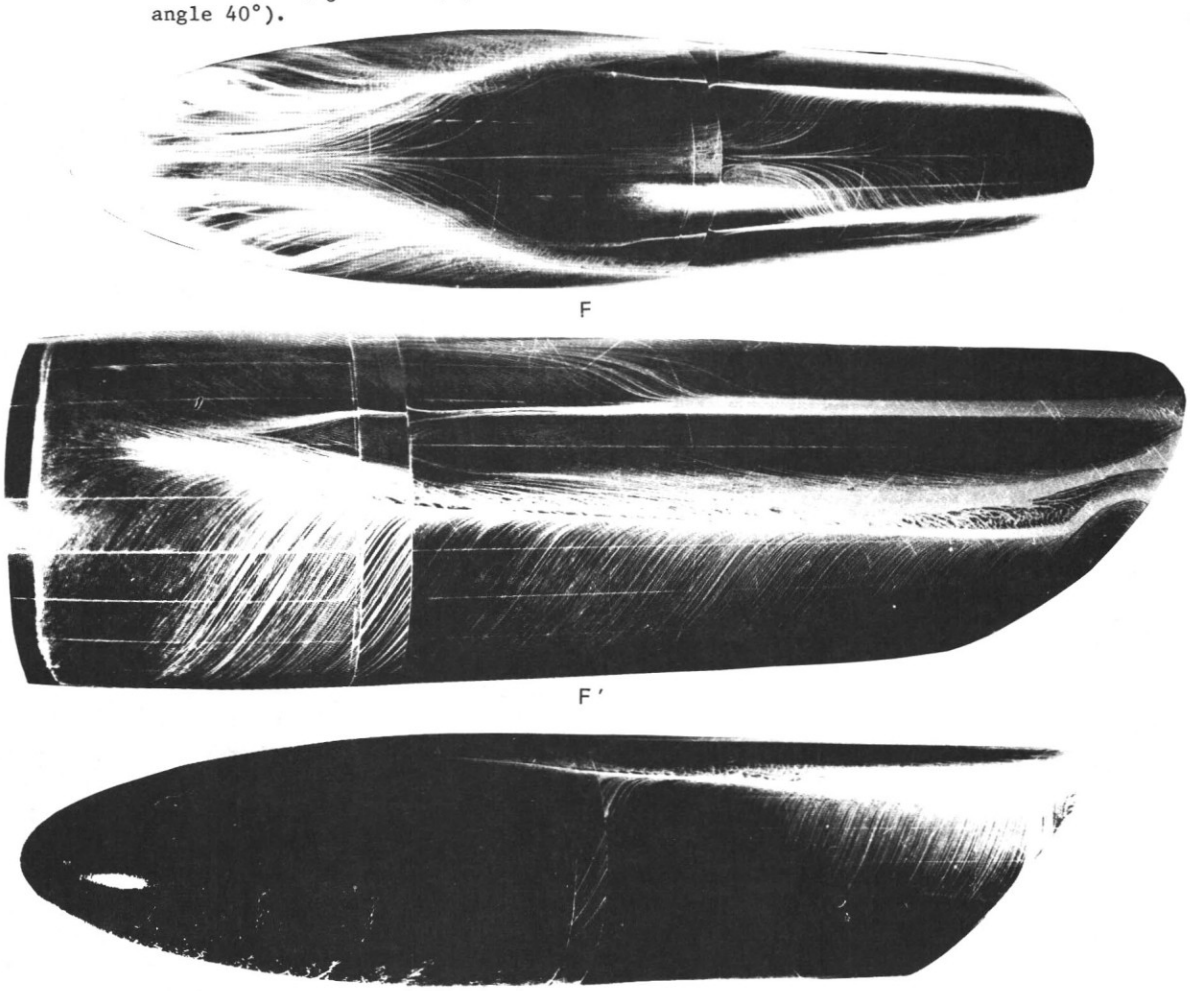

Figure 17. Photographies of flow lines (V_o = 90m/s, pitch angle 40°).

The figure 18 schematizes this complex flow, contributes to the understanding of the photographies and shows a sketching of the flow in a plane perpendicular to the axis (abscissa X/L = 0.48). On this drawing S_1, S_2, A_2 are obtained thanks to the photographies, but the external flow lines are conjectural.

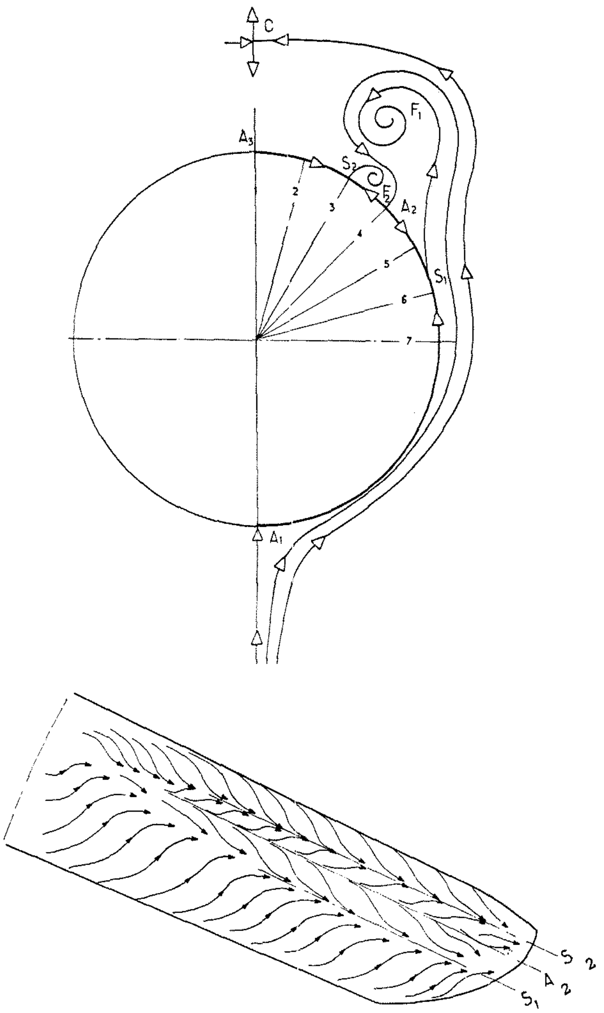

Figure 18. Sketch of the flow.

V.3. Wake Survey Of a Fighter

An old model of Mirage G8, scale 1/8.6 was used for detailed study of the near wake with the laser velocimetry. The aim of this test is a better understanding of the causes producing the drag. So the experimental results will be a good help to validate computation of tridimensionnal wakes.

The complete model is in the wind tunnel with the vertical of the fighter in the horizontal plane of the test section containing the axis of the wind tunnel. The model is fixed, by an horizontal swept-back mast, to the right wall of the wind tunnel. The incidence is 5 degrees. Due to the position of the model in the test section, the laser velocimeter measures : u parallel to u_∞ and to the X axis of the wind tunnel, v perpendicular to the plane of symmetry of the airplane, so $\sqrt{\overline{u'^2}}$ and $\sqrt{\overline{v'^2}}$.

The wake is studied in a plane located 0.3 m behind the base of the model ; this plane, 1.5 m along the span, 1 m along the airplane vertical (the wind tunnel horizontal), is explored along 29 horizontal lines (100 measurements by line) with an interval of 0.05 m along the span.

The figure 19 (a,b,c,d), shows the lines iso u, iso v, iso $\sqrt{\overline{u'^2}}$, iso $\sqrt{\overline{v'^2}}$. The wake of each component appears clearly, the image of the two vortices is characterized by the inversion of the transverse speed v and large fluctuations. The images of these vortices are well designed by the distribution of the module of the speed (v) in the explored plane (figure 19e).

The same exercise was made on three lines located at 0.002, 0.102 and 0.202 m behind the leading edge.

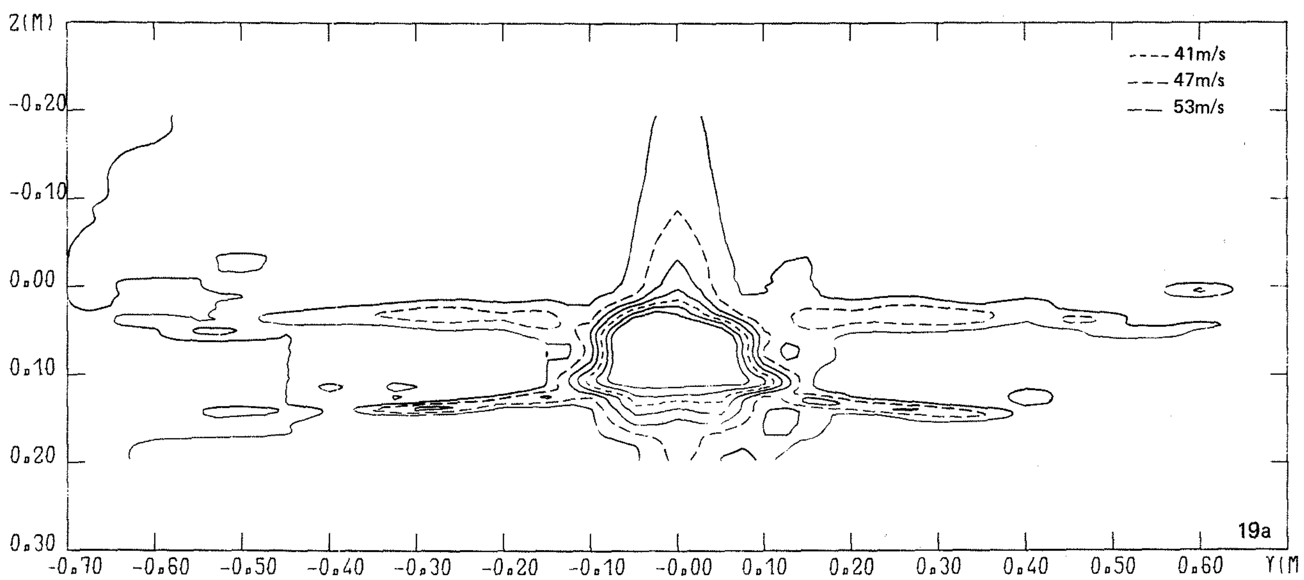

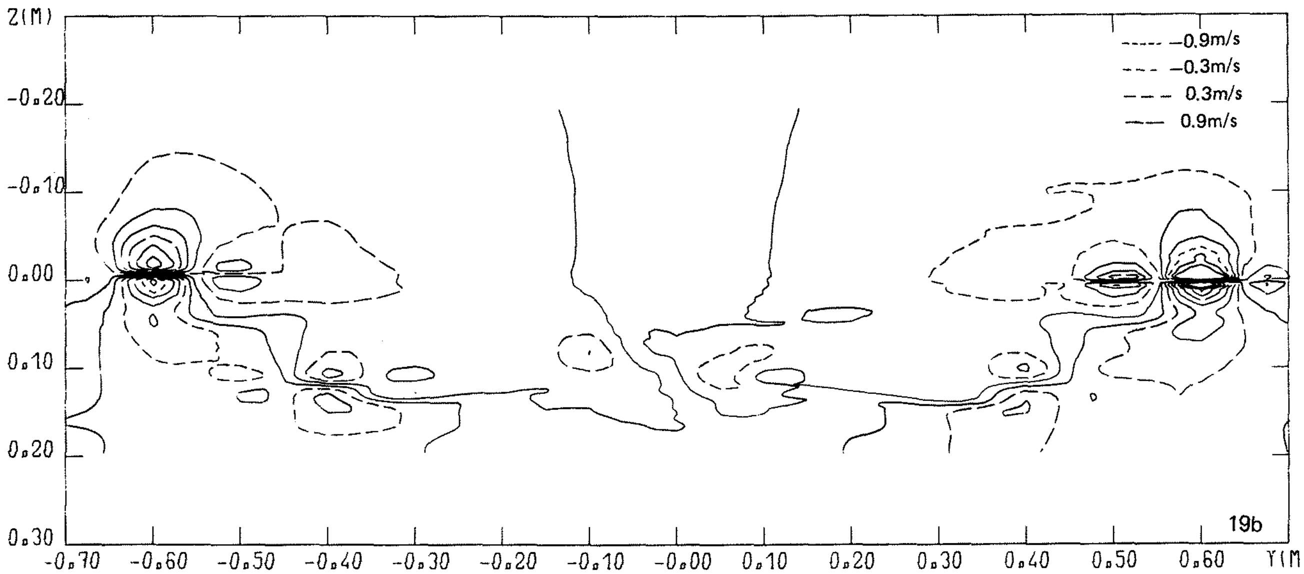
Z(M)
-0.20
-0.10
0.00
0.10
0.20
0.30
-0.9m/s
-0.3m/s
0.3m/s
0.9m/s
19b
-0.70 -0.60 -0.50 -0.40 -0.30 -0.20 -0.10 -0.00 0.10 0.20 0.30 0.40 0.50 0.60 Y(M)

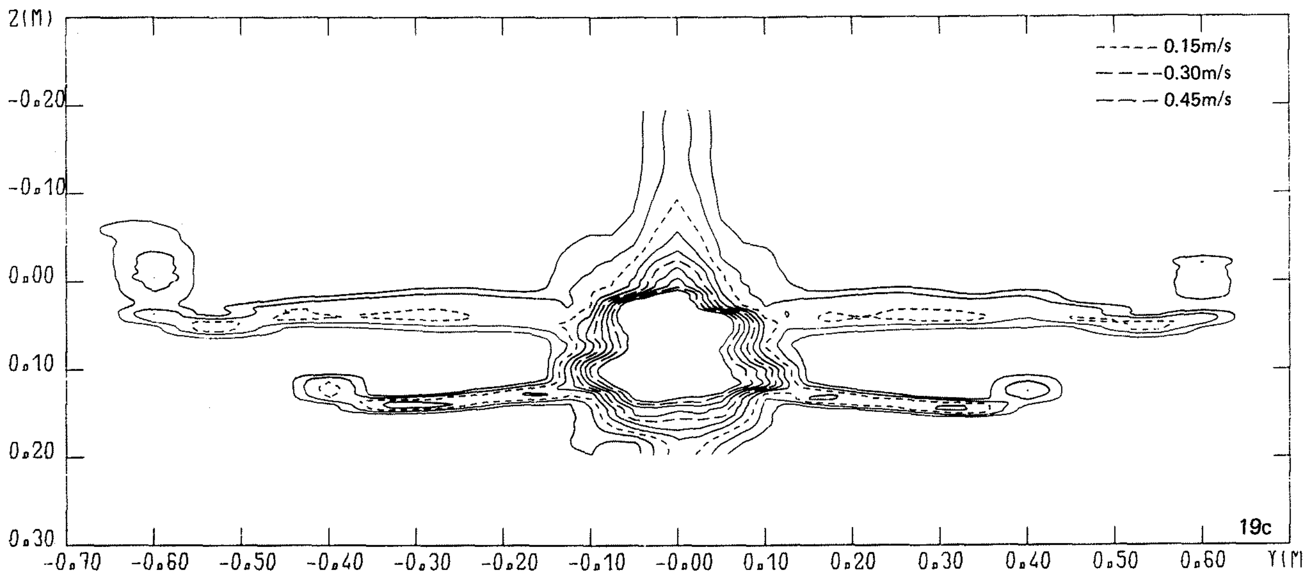
Z(M)
-0.20
-0.10
0.00
0.10
0.20
0.30
0.15m/s
0.30m/s
0.45m/s
19c
-0.70 -0.60 -0.50 -0.40 -0.30 -0.20 -0.10 -0.00 0.10 0.20 0.30 0.40 0.50 0.60 Y(M)

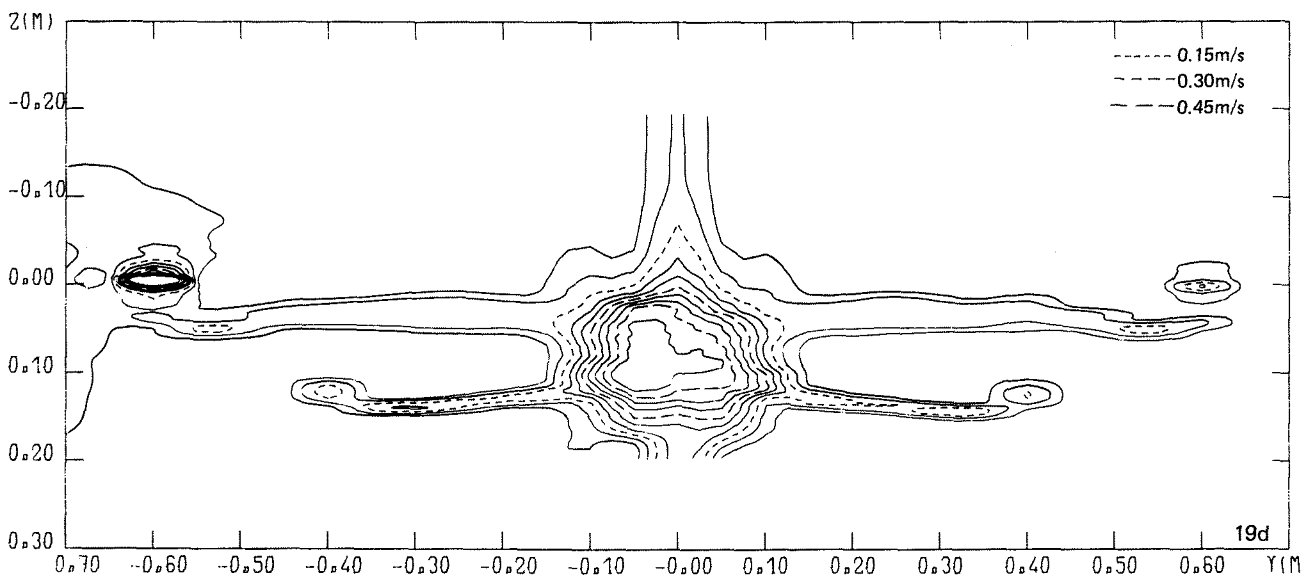
Z(M)
-0.20
-0.10
0.00
0.10
0.20
0.30
0.15m/s
0.30m/s
0.45m/s
19d
0.70 -0.60 -0.50 -0.40 -0.30 -0.20 -0.10 -0.00 0.10 0.20 0.30 0.40 0.50 0.60 Y(M)

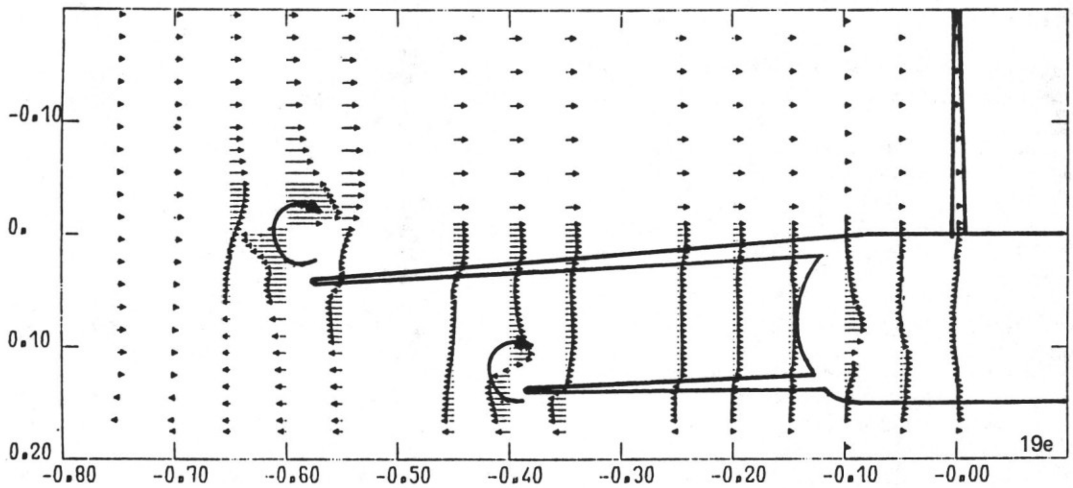

Figure 19. Wake survey with laser velocimeter (19a iso u, 19b iso v, 19c iso u', 19d iso v', 19c transversal speed v. On these figures continuous lines between dotted lines are equally spaced, for example on 19a between 41m/s and 47m/s we show 43m/s and 45m/s).

V.4. Flat Delta Wing

The tests on a flat delta wing are devoted to a better understanding of the birth, the development and the breakdown of vortices on this type of airfoil.

The figure 20 shows the flow visualized by oil at Vo = 40 m/s and pitch angle 30 degrees. This 75 degrees swept angle wing is defined by length 1.45 m, semi span 0.3885 m.

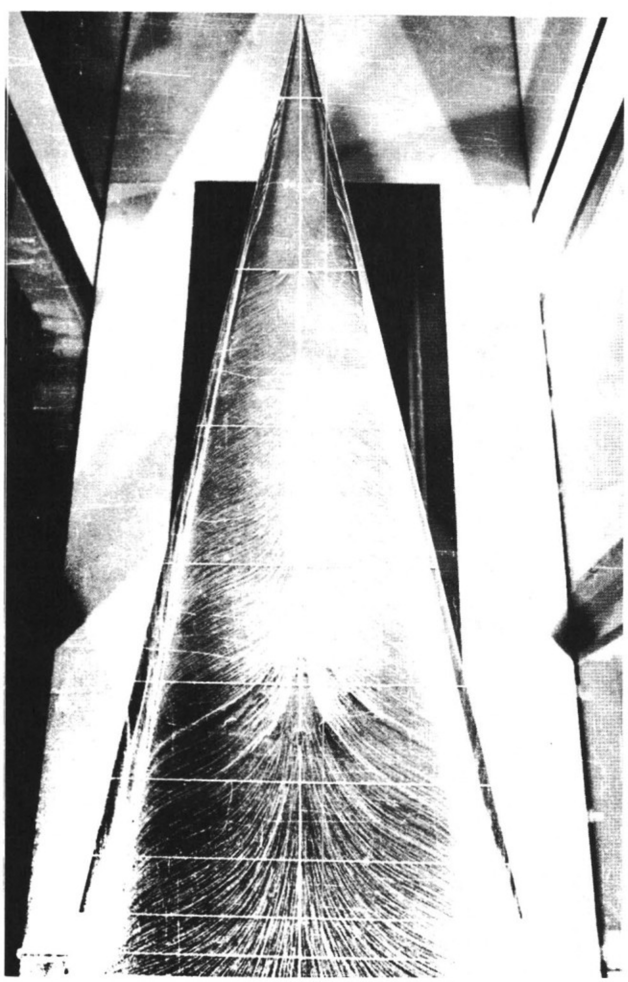

Figure 20. Flow lines on the 75 degree swept wing (40m/s, 30°).

The distribution of Cp (or Kp), the pressure coefficient, is given in figure 21 at V = 40 m/s, 30 degrees and V = 40 m/s, 15 degrees

A lecture "Leading edge vortex flow over 75 degrees swept delta wing, experimental and computational results", will be given on this subject by Manie, Pagan, Solignac and Carcaillet. So I will stop here.

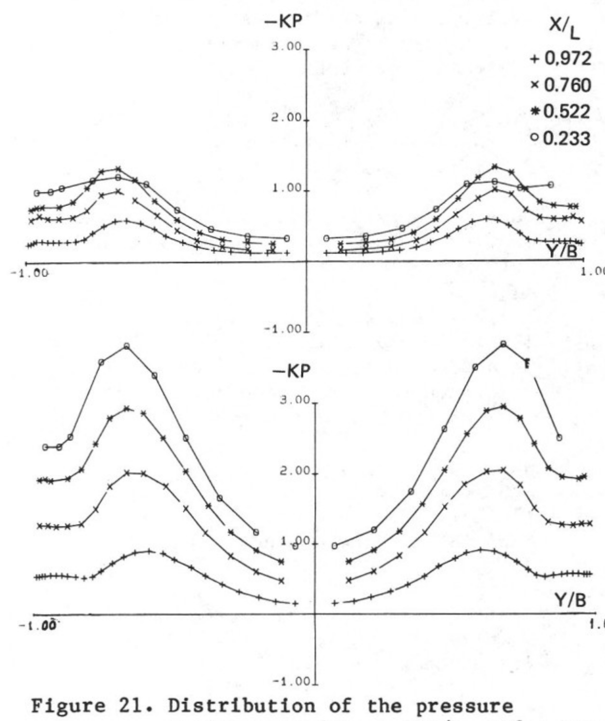

Figure 21. Distribution of the pressure coefficient (21a : 40m/s, 15° ; 21b 40m/s, 30° ; B is local semi span, L the lenght 1.45m, X and Y the coordinates)

VI. Conclusion

We have described the research wind tunnel F_2 and its capabilities.

Some examples taken out of the tests have illustrated these capabilities.

The results obtained today encourage to continue the improvement of the measurement equipment, intrusive and non intrusive, and to develop a good cooperation with the specialist of flow modeling.

I am pleased to thank Mr Afchain in charge of F_2 and his assistants and MM.Boutier, Delery, Gleizes, Solignac who allowed me the use of their results.

References

(1) NASA
Future computer requirements for computational aerodynamics
NASA CP 2032, 1978.

(2) Chapman, D.R.
Computational aerodynamics - Development and outlook
AIAA Journal Vol 17, Dec 1979, pp 1293 - 1313.

(3) Heinzerling, W.
A critical comparison between wind tunnel and supercomputer with respect to their performance and cost effectiveness for complex aerodynamic simulation of high quality in aircraft development (DGLR lecture n°82-051) Annual meeting of the DGLR Stuttgart, oct 1982.

(4) Tidjeman, H.
On the role of computational fluid dynamics in aerodynamic research and development.
Paper presented during the 17 th Israel conference on mechanical engineering, Tel Aviv university July 12-14 1983.

(5) National Research Council
The influence of computational fluid dynamics on experimental aerospace facilities. A fifteen year projection. National Academy Press - Washington 1983.

(6) NASA
NASA Computer science research program plan
NASA Technical memorandum 85631, 1983.

(7) Perrier, P.
L'aérodynamique et les aérodynamiciens de l'an 2000
Air et Cosmos Special 1000 - 5 mai 1984.

(8) Snyder, C.T. and Presley L.L.
Current wind tunnel capability and planned improvements at NASA
Ames research center.
AIAA-86-0729-CP AIAA 14 th Aerodynamic testing conference March
5-7, West Palm Beach, Florida 1986.

(9) Marvin, J.G.
Future requirements of wind tunnel for computational fluid dynamics code verification.
AIAA-86-0752-CP AIAA 14 th Aerodynamic testing conference March 5-7, West Palm Beach, Florida 1986.

(10) Une Nouvelle Soufflerie au FAUGA-MAUZAC
Air et Cosmos n°960 - 25 juin 1983.

(11) French test laser sitted wind tunnel
Aviation Week - July 18, 1983.

(12) Afchain.D, Broussaud.P, Frugier.M, Rancarani.G,
La soufflerie F2 du Centre du Fauga-Mauzac. 20e colloque d'aérodynamique appliquée AAAF Toulouse 8-10 novembre 1983
T.P. ONERA n°1983-139.

(13) Boutier.A, Canu.M,
Application of laser velocimetry to large industrial wind tunnels
International Symposium of Applications of laser Doppler Anemometry to Fluid Mechanics, Lisbonne 5-7 july 1982 ONERA T.P n°1982-63

(14) Boutier.A, Haziza.E, Lefebvre.D, Lefebvre.J
New applications of laser velocimetry in ONERA wind tunnels.
10 th ICIASF, Saint Louis 20-23 september 1983.
ONERA T.P. n°1983-114

(15) Boutier.A, D'Humières.CH, Soulevant.D,
Three dimensional Laser Velocimetry : a review.2 nd International Symposium on "Applications of laser anemometry to fluid mechanics". Lisbonne 2-4 july 1984.
ONERA T.P. n° 1984-43

(16) Boutier.A,
Laser velocimetry and wall approach limitations. International laser Anemometry Symposium.
Miami 17-21 november 1985
ONERA T.P. n° 1985-155

(17) Boutier.A, Pagan.D, Soulevant.D,
Measurements accuracy with 3D laser velocimetry
International conference on laser anemometry, adavances and application.
Manchester 16-18 december 1985.
ONERA T.P. n°1985-71.